NUCL SCI TECH (2016)27:113
DOI 10.1007/s41365-016-0111-9

A data-based photonuclear simulation algorithm for determining specific activity of medical radioisotopes

Wen Luo[1,2] · Dimiter L. Balabanski[2] · Dan Filipescu[2]

Received: 28 January 2016 / Revised: 15 May 2016 / Accepted: 21 May 2016

Abstract For simulating more accurately neutron or proton production from photonuclear reactions, a data-based photonuclear reaction simulation algorithm has been developed. Reliable photonuclear cross sections from evaluated or experimental database are chosen as input data. For checking the validity of the use of the data-based photonuclear algorithm, benchmarking simulations are presented in detail. We calculate photonuclear cross sections or reaction yield for ^{9}Be, ^{48}Ti, ^{133}Cs, and ^{197}Au and compare them with experimental data in the region of incident photon energy below $\sim$30 MeV. While Geant4 can hardly reproduce photonuclear experimental data, results obtained from the data-based photonuclear algorithm are found in good agreement with experimental measurements. Potential application in estimation of specific activity of radioisotopes is further discussed. We conclude that the developed data-based photonuclear algorithm is suitable for an accurate prediction of photon-induced neutron or proton productions.

This work was supported by the National Natural Science Foundation of China (Nos. 11405083 and 11675075), the Young Talent Project of the University of South China and the Extreme Light Infrastructure—Nuclear Physics (ELI-NP)—Phase I, a project co-financed by the European Union through the European Regional Development Fund.

✉ Wen Luo
wenluo-ok@163.com

[1] School of Nuclear Science and Technology, University of South China, Hengyang 421001, China

[2] Extreme Light Infrastructure - Nuclear Physics (ELI-NP)/ "Horia Hulubei" National Institute for R&D in Physics and Nuclear Engineering (IFIN-HH), 30 Reactorului St., Bucharest-Magurele, jud. Ilfov, P.O.B. MG-6, 077125 Iasi, Romania

Keywords Medical radioisotope · Photonuclear simulation · Photon–neutron · Photo-proton · Specific activity · Geant4

1 Introduction

Photonuclear reactions and the resulted neutron or proton productions play an important role in studies of the astrophysical process [1–3], long-lived nuclear waste transmutation [4–7], photon-induced activation analysis [8–10], radioisotope production [11–15], boron neutron capture therapy (BNCT) [16, 17], and radiography as well as radiotherapy [18–20]. Photonuclear reactions have demonstrated their potential in production of radioisotopes of medical interest by (γ, n) reactions, but a high-energy photon beam of high-flux density is generally required. Such photon beam could be produced with either an electron linear accelerator (linac) [11, 12] or a Compton backscattering (CBS) γ-ray facility [21, 22]. Concerning production of medical radioisotopes using photonuclear reactions, it is crucial to estimate accurately photo-neutron or photo-proton yield and then to obtain reliable specific activity of the produced radioisotopes.

Currently, Geant4 [23, 24], FLUKA [25], and MCNP are common Monte Carlo simulation tools useful for photonuclear studies. Geant4 includes comprehensive physics processes and databases of particle matter interactions and has been regarded as a good platform to facilitate the studies mentioned above. In order to check the validity of Geant4 (v4.9.6.03) for this purpose, we simulated (γ, n) and (γ, 2n) reaction cross sections and compared them with experimental data in the EXFOR database [26]. Usually, photonuclear cross sections have broad

Published online: 27 August 2016

peaks with relatively high values in the giant dipole resonance (GDR) energy region [26], i.e. $E_\gamma \leq 30$ MeV. Therefore, the studies within the GDR region have received much attention. However, the hadronic model existing in Geant4 cannot reproduce experimental photonuclear cross sections [27, 28]. In particular, for peaked GDR cross sections, a large discrepancy existed in Geant4 simulations and measurements. Without accurate simulation of them, photon-induced neutron or proton productions can hardly be described and the resultant yield estimations are not reasonable. In order to address these issues, a data-based photonuclear reaction model for Geant4 has been demonstrated [28].

Similar to Ref. [28], we demonstrated in this work a data-based photonuclear reaction simulation algorithm for an accurate simulation of the photon-induced neutron or proton production by considering reliable photonuclear cross sections and photon attenuation effect inside the target. The developed simulation algorithm was verified to accurately reproduce experimental photonuclear cross sections as well as reaction yields. Then, it was used to predict specific activity of several medical radioisotopes, which could be produced at the extreme light infrastructure-nuclear physics (ELI-NP) facility [21] for research in nuclear medicine. The data-based simulation algorithm is given in Sect. 2. Benchmarking simulations and results obtained from the simulation algorithm are shown in Sect. 3. Section 4 reviews potential application in estimation of specific activity of radioisotopes. Conclusion and outlook are given in Sect. 5.

2 Methods

2.1 Specific activity of radioisotope

The specific activity (A/m) is one of the most important quality criteria for radioisotopes production in nuclear medicine research and application and usually expressed in GBq/mg, Ci/mg (= 10^6 mCi/g) or similar units. Here, A is the activity, and m stands for the mass. The theoretical maximum specific activity for a pure radioisotope without admixture of stable isotopes is given by:

$$\left(\frac{A}{m}\right)_{\max} = \frac{\lambda_1 N_A}{M}, \tag{1}$$

where $\lambda_1 = \ln(2)/T_{1/2}$ is the decay constant of the product isotope with the half-life $T_{1/2}, M$ is the molar mass (g/mol) of the target isotope, and $N_A = 6.02\times\ 10^{23}$ represents Avogadro's constant.

When an intense γ-beam transmutes a target isotope into the desired product, and considering that any other reactions (such as destruction of the product by nuclear reactions) do not interfere significantly, the achievable specific activity is given by:

$$\left(\frac{A}{m}\right)_{\text{product}} = \frac{Y}{m}(1-a). \tag{2}$$

Here, Y is the reaction yield for transmutation of the target into the product, the variable a is expressed as $a = \exp(-\lambda_1 t_{\text{irr}}),$, and t_{irr} is the irradiation time. Equation (2) shows that to obtain a reliable reaction yield enables further accurate calculation of specific activity. For some specific cases, the daughter of the product isotope, rather than itself, is of particular interest in nuclear medicine application and the product isotope is only used as a radionuclide generator. A typical example is the ^{99}Mo/^{99m}Tc generator, which is usually produced by a neutron-induced fission process, or by photo-neutron reaction and its disintegration, $^{100}\text{Mo}(\gamma,\text{n})^{99}\text{Mo} \rightarrow {}^{99m}\text{Tc}$. For the latter, we derived the specific activity of the daughter radionuclide from the decay law:

$$\left(\frac{A}{m}\right)_{\text{daughter}} = \frac{Y}{m}(1+b), \tag{3}$$

where λ_2 corresponds to the decay constant of the daughter radioisotope, and the variable b is given by

$$b = \frac{\lambda_1 \exp(-\lambda_2 t_{\text{irr}}) - \lambda_2 \exp(-\lambda_1 t_{\text{irr}})}{\lambda_2 - \lambda_1}. \tag{4}$$

When the generator radioisotope has a smaller decay constant than that of the daughter radioisotope, a radioactive decay equilibrium between them could be reached. Then, one could optimize the irradiation time to obtain achievable specific activity for the daughter radioisotope.

2.2 Monte Carlo simulation algorithm for photonuclear reaction

High-energy photons with appropriate energy, e.g. 10–30 MeV, can excite mainly through GDR mechanism, the target nuclide. The excited nuclide will decay primarily through emitting a nucleon (proton or neutron) or a photon. Such a process is usually designated as the photonuclear process, by which an activated daughter nuclide is generated. In order to produce medical radioisotopes, an interesting case is through ejecting a single neutron or proton, a so-called photo-neutron and photo-proton production process.

In a typical photonuclear process, reaction yield Y depends upon a number of parameters, such as number density, ρ, of target nuclei that are irradiated, threshold energy of nuclear reaction, E_{th}, end-point energy of γ-rays, $E_{\max}$, probability of photonuclear reaction defined by reaction cross section, σ_{E_γ}, and γ-ray flux density. While taking into account attenuation

coefficient of γ-photons inside target, reaction yield can be written as:

$$Y = \int_{E_{\text{th}}}^{E_{\max}} \int_0^R \frac{\rho \cdot N_{\text{A}}}{M} \frac{\sigma(E_\gamma)}{\mu(E_\gamma)} I(E_\gamma, r) \times [1 - \exp(-\mu(E_\gamma) \cdot L)] \mathrm{d}E_\gamma \mathrm{d}r, \quad (5)$$

where M is the molar mass (g/mol) of the target isotope, $I(E_\gamma, r)$ is the γ-ray linear flux density at the surface of the target after the polar-angle integration, $\mu(E_\gamma)$ is the linear attenuation coefficient, R is the cylindrical target radius, and L is the target thickness with respect to the direction of γ-beam propagation. Due to the γ-ray attenuation inside the target, γ-ray flux decreases as target thickness increases. It should be noted that photons scattered inside the target may cause photonuclear reactions. However, the occurrence of such phenomenon depends basically on the radius of the target. For a target with a large radius, the change of the photon energy and of the angle should be included in the following simulation. Conversely, for a target with a relatively small radius, the effect of scattered photons that trigger photonuclear processes could be neglected, even if the target is very thick. This is attributed to the scattered photons that stray from the direction of incidence, and, as a result, they can easily escape from the target along lateral direction. In our simulation, small radius target is used and accordingly we did not consider the effect discussed.

For a certain geometry of irradiated target, we sampled a certain γ-photon with energy, $E_{\gamma,i}$, and position, r_i, which is recorded at the surface of the target. Accordingly, the cross section, $\sigma_i(E_{\gamma,i})$, and the attenuation coefficient, $\mu_i(E_{\gamma,i})$, were obtained using a linear interpolation method. Based on Eq. (5), we calculated the reaction probability for the ith γ-photon at position r_i interacting with the isotope inside the target as:

$$p_i = \begin{cases} \frac{\rho \cdot N_{\text{A}}}{M} \frac{\sigma_i(E_{\gamma,i})}{\mu_i(E_{\gamma,i})} [1 - \exp(-\mu_i(E_{\gamma,i}) \cdot L)] & \text{if } \mathrm{r_i} \leq \mathrm{R}, \\ 0 & \text{if } \mathrm{r_i} > \mathrm{R}. \end{cases} \quad (6)$$

Further, we obtained the reaction yield to be:

$$Y = \frac{I}{N} \sum_{i=1}^{N} p_i. \quad (7)$$

Here, I is the incident photon flux at the surface of the isotopic target, and N is the total sampling number. By substituting Eq. (7) into Eqs. (2) and (3), one could obtain specific activity of produced radioisotope and its daughter radionuclide as:

$$\left(\frac{A}{m}\right)_{\text{product}} = \frac{I}{\pi R^2} \cdot \frac{N_{\text{A}}}{M} \cdot (1 - a) \cdot \frac{1}{N} \sum_{i=1}^{N} \sigma_i(E_{\gamma,i}) \frac{1 - \exp(-\mu_i(E_{\gamma,i}) \cdot L)}{\mu_i(E_{\gamma,i}) \cdot L}, \quad (8)$$

and

$$\left(\frac{A}{m}\right)_{\text{daughter}} = \frac{I}{\pi R^2} \cdot \frac{N_{\text{A}}}{M} \cdot (1 + b) \cdot \frac{1}{N} \sum_{i=1}^{N} \sigma_i(E_{\gamma,i}) \frac{1 - \exp(-\mu_i(E_{\gamma,i}) \cdot L)}{\mu_i(E_{\gamma,i}) \cdot L}. \quad (9)$$

2.3 γ-beam characteristics simulation

As presented above, there are two main approaches for production of high-energy γ-beams of high intensity. One is through bremsstrahlung process based on linac, and another is via the Compton backscattering of a laser light off a very brilliant and intense electron beam. While Geant4 toolkit is well defined to predict the beam characteristics stemmed from the bremsstrahlung mechanism, several laser-Compton scattering simulation codes [29–32], benchmarked against experimental data produced by worldwide CBS γ-ray facilities, have been developed. These codes are suitable to model the MeV-class γ-ray production and to study the spectral and flux density distributions of the γ-beam during its transport from the laser-electron interaction point (IP) to the target, through the CBS γ-ray beamline. These parameters will be taken as input data, to facilitate calculation of photonuclear reaction yield and specific activity of desired radioisotopes.

2.4 Photonuclear cross section and γ-ray attenuation coefficient calculation

In order to obtain the reaction yield shown in Eq. (5), reliable photonuclear cross sections are estimated (or measured) and γ-ray attenuation coefficient for a certain target isotope is required. While acquiring photonuclear cross sections from EMPIRE calculation [33] and from TENDL evaluation [34], we can also cite experimental ones available in the EXFOR database [26]. If possible, a detailed comparison between them will be conducted, which enables us to select prudently photonuclear cross sections. For incident photons covering energy from 1 keV to 20 MeV, the mass attenuation coefficients are available in Ref. [35]. Then, the linear attenuation coefficient required by Eqs. (5) and (6) could be obtained readily. As the irradiated target with compound and mixture are employed, the linear attenuation coefficient is reprocessed according to its content and composition. Further, since the set of data for the photonuclear reaction and attenuation coefficient were popularly discrete, we used linear interpolation method to calculate their values for incident γ-rays with arbitrary energy.

According to above simulation and calculation algorithms, a data-based Monte Carlo simulation C++ program, integrated with Geant4, or Geant4-based γ-beam simulation code [30–32], was developed for determining photonuclear isotope production, induced by a high-intensity γ-ray beam either from linac-based bremsstrahlung source or from CBS-driven γ-ray facility. Since the prudent photonuclear cross section, flexible incident photon beam, and attenuation effect inside irradiated target were fully considered, it can be easily used to investigate the effects of incident γ-beam and target geometric parameters on photonuclear yield and consequently to predict specific activity of radioisotopes. In the following, several benchmarking simulations will be given in order to check the validity of the use of the data-based simulation algorithm.

3 Results and discussions

3.1 Benchmarking simulations

As presented in the Introduction, Geant4 can be used to simulate photonuclear processes. To check the validity of the photonuclear model existing in Geant4, we have first simulated photonuclear reaction cross sections and compared them with experimental data provided by the EXFOR database [26]. For photonuclear interactions, Geant4 popularly uses the "G4PhotoNuclearProcess" class [36]. It handles inelastic photon scattering from nuclei by invoking one or more hadronic models and one or more hadronic cross sections. In our case, the Bertini intra-nuclear cascade model, i.e. the "G4CascadeInterface" class, was invoked. It was used to simulate final states for photonuclear reactions. Although the model is available for the region of incident photon energy $0 \leq E_\gamma < 3.5\,\text{GeV}$ in Geant4, it has only been tested in a energy range $60\,\text{MeV} \sim 3\,\text{GeV}$ [37].

Simulations of photon-induced neutron production were performed for ^{9}Be,^{133} Cs, and ^{197}Au. ^{9}Be is a one of the light nuclei, and its target material is useful for producing photo-neutrons while using low-energy bremsstrahlung radiation because of a very low neutron separation energy ($E_{\text{th}} \sim 1.66\,\text{MeV}$). ^{133}Cs is a suitable candidate in an intermediate mass region due to a considerable reaction cross section. ^{197}Au is suitable for the production of large amounts of neutrons due to a high reaction cross section. To compute photonuclear reaction cross sections, we used a cylindrical target with 1.0 mm thick and 4.5 cm radius arbitrarily for representing a "semi-infinite geometry". For brevity, the results obtained from the Geant4 with the "G4PhotoNuclearProcess" class are hereafter simply referred to as "G4PNP". As a comparison, many experimental data in the EXFOR database [26] were used, and the data will hereafter be simply referred to as "EXFOR".

Figure 1 shows the comparison of G4PNP with EXFOR for $^{9}\text{Be}(\gamma, \text{n})$ and $^{9}\text{Be}(\gamma, 2\text{n})$ reaction crosssections in the GDR region of incident photon energy $E_\gamma \leq 35\,\text{MeV}$. Large discrepancies can be observed between the G4PNP simulations and EXFOR data for (γ, n)E reaction crosssection in the GDR region. For $^{9}\text{Be}(\gamma, \text{n})$ reaction, the model of G4PNP does not reproduce the low-energy peaks of the cross section and underestimates the experimental cross section by up to $\sim 10^3$ in the region of incident photon energies $E_\gamma < \sim 15\,\text{MeV}$. Such discrepancy is attributed to an underestimation of neutron production for $^{9}\text{Be}(\gamma, \text{n})$ reaction, as discussed later. The cross section on $^{9}\text{Be}(\gamma, 2\text{n})$ underestimates the experimental value in the peak region by a factor of 10.

A similar feature for the underestimation of cross sections can also be seen in the case of $^{133}\text{Cs}(\gamma, \text{n})$ and $^{197}\text{Au}(\gamma, \text{n})$ reactions. Figure 2a, c shows that both the $^{133}\text{Cs}(\gamma, \text{n})$ and $^{197}\text{Au}(\gamma, \text{n})$ cross-sectional peak values given by the G4PNP are lower than the experimental ones. The comparisons of G4PNP with EXFOR for $^{133}\text{Cs}(\gamma, 2\text{n})$ and $^{197}\text{Au}(\gamma,2\text{n})$ reaction cross sections in the GDR region are plotted in Fig. 2b, d, respectively. While the G4PNP cross section on $^{197}\text{Au}(\gamma,2\text{n})$ is very close to experimental

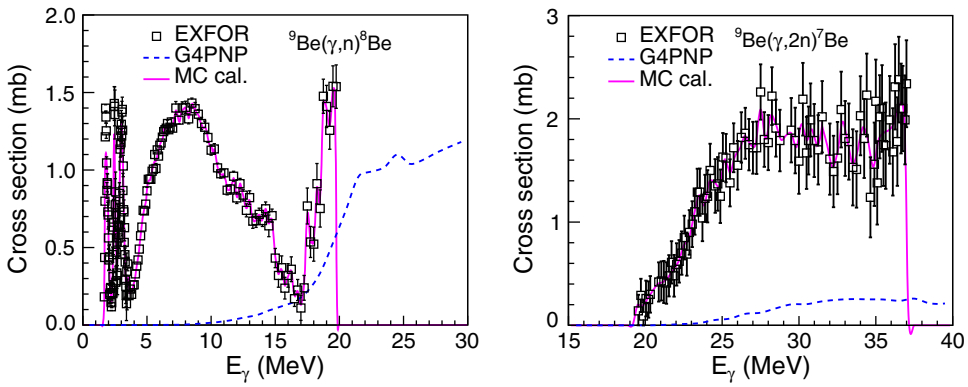

Fig. 1 (γ, n) and $(\gamma, 2\text{n})$ reaction cross sections for ^{9}Be as a function of incident photon energy. The *open squares* are the experimental data taken from the EXFOR database [26]. The *solid lines* and the *dashed lines* represent the results obtained from the data-based Monte Carlo calculations and Geant4 simulations using G4PhotoNuclearProcess, respectively

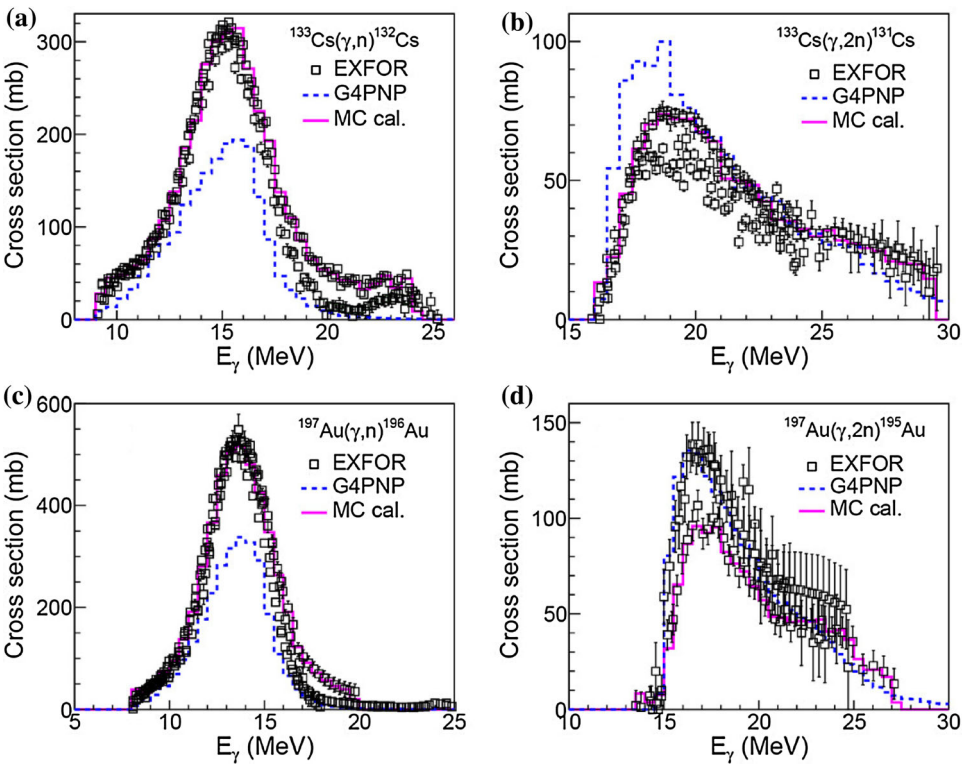

Fig. 2 (γ, n) reaction cross sections for ^{133}Cs (**a**) and ^{197}Au (**c**), and $(\gamma, 2\mathrm{n})$ reaction cross sections for ^{133}Cs (**b**) and ^{197}Au (**d**) as a function of incident photon energy. The *open squares* are the experimental data taken from the EXFOR database [26]. The *solid lines* and the *dashed lines* represent the results obtained from the data-based MC cal. and Geant4 simulations using G4PhotoNuclearProcess, respectively

data, the value on ^{133}Cs(γ,2n) (100 mb) overestimates the experimental cross section (74.9 $\pm$ 1.8 mb) in the peak region by a factor of 1.3.

Comparisons with experimental data for photo-proton reactions are performed as well. Taking $^{48}\mathrm{Ti}(\gamma, \mathrm{p})^{47}\mathrm{Sc}$ as an example, the simulated results from G4PNP diverge from the data available in the EXFOR database (see Fig. 3). Through the above comparisons, it is found that Geant4 (v4.9.6.03) can hardly reproduce the experimental photonuclear reaction cross sections in the GDR region, which is also verified by a similar comparison in Ref. [28]. Hence, it is necessary to develop an alternative approach for simulation of photonuclear reaction in this low energy region.

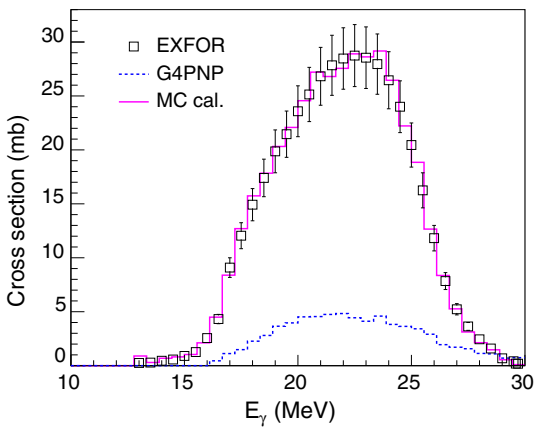

Fig. 3 Simulation of reaction cross sections on ^{48}Ti(γ,p) as a function of incident photon energy. The *open squares* are the experimental data taken from the EXFOR database [26]. The *solid lines* and the *dashed lines* demonstrate the results given by the data-based MC cal. and Geant4 simulations, respectively

3.2 Data-based Monte Carlo simulation for photonuclear reaction

To check the validity of the developed algorithm demonstrated in Sect. 2, we also performed the same simulations for photonuclear reactions on ^{9}Be,^{133}Cs, and ^{197}Au. The data-based Monte Carlo calculations (simply referred to as MC cal.) for both (γ, n) and $(\gamma, 2\mathrm{n})$ reaction cross sections of ^{9}Be,^{133}Cs, and ^{197}Au are shown in solid lines of Figs. 1 and 2. It is found that there is good agreement between the calculated results and EXFOR for photo-neutron production cross sections. Although the predicted $^{9}\mathrm{Be}(\gamma, \mathrm{n})$ and ^{9}Be(γ,2n) reaction cross sections by using G4PNP differ from the experimental ones by a factor of $10 - 10^3$, the cross sections from the MC cal. are very close to those of the EXFOR. In addition, it describes well the low energy resonance structure of the $^{9}\mathrm{Be}(\gamma, \mathrm{n})$ presented in Fig. 1a. For photo-neutron cross sections of the ^{133}Cs and ^{197}Au, the detailed comparisons show that the predictions from the data-based MC cal. are in good

agreement with the experimental data. Figure 3 shows the simulation of photo-proton cross sections on the ^{48}Ti with experimental data. It demonstrates that the simulated results are in accordance with the experimental data.

To substantiate the use of the new developed code, benchmark simulations were performed for photonuclear reaction yield from the $^{9}\mathrm{Be}(\gamma,\mathrm{n})$ reaction. The photons used to trigger the reaction were generated from a 8.96 MeV electron beam (e-beam) impinging on a 1.88-mm tantalum target through the bremsstrahlung process [38, 39]. The photo-neutron yield with respect to the thickness of the beryllium target is shown in Fig. 4. The yields calculated using the data-based simulation code, and the G4PNP are compared with the experimental data [38]. Calibrated SSNTD CR-39 films and Silver wrapped GM detectors were used for the experimental measurements. Since the experimental data taken from CR-39 films were in accordance with that from GM detector within 10 % [38], the data used for the benchmarking should be reliable.

The results taken from the data-based MC cal. were in accordance with the experimental data for different volumes of beryllium target. The calculation point at 8 cm overestimated the experimental one. This could be readily understood in that the bremsstrahlung photons emitted (and then recorded at the surface of the beryllium target) had a relatively large angular distributions. However, a parallel bremsstrahlung photon beam was assumed for simulation, to irradiate the target. It meant that the number of the bremsstrahlung photons, used to induce photon–neutron reactions, was overestimated slightly, and the photo-neutron reaction yield was enhanced accordingly. Large discrepancies between the results from the G4PNP calculations and the experimental measurements are observed in Fig. 4. The G4PNP underestimates the photo-neutron yields by three orders of magnitude since the model cannot reproduce the experimental $^{9}\mathrm{Be}(\gamma,\mathrm{n})$ reaction cross section as shown in Fig. 1a. This benchmark simulation shows that the data-based simulation code gives reasonable results for photonuclear reaction yield calculations in the GDR region. As a consequence, the validity of the data-based simulation algorithm was justified.

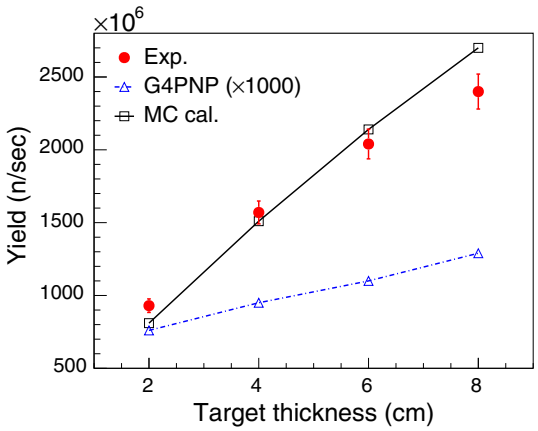

Fig. 4 Photonuclear reaction yield from beryllium target as a function of the target thickness. The *filled circles* are the experimental data from [38]. The *squares* with a *solid line* and the *triangles* with a *dashed line* represent the photonuclear reaction yields obtained from data-based calculation and Geant4 simulation using the G4PhotoNuclearProcess, respectively

4 Estimation of specific activity for radioisotopes of medical interest at ELI-NP

CBS γ-beams of high intensity deliver several unique features to produce photonuclear isotopes production [40]. The upcoming facility ELI-NP is expected to provide a brilliant γ-beam, very intense (up to 10^{13} photons/s), $\leq 0.5\,\%$ bandwidth, with $E_\gamma > 19$ MeV, which is obtained by incoherent Compton backscattering of a laser light off an intense, classical e-beam ($E_e > 700$ MeV) produced by a warm linac [21]. This shall provide an unprecedented possibility for the production of radioisotopes in sufficient quantities for nuclear medicine research. The production of several radioisotopes, using photonuclear reaction mechanism, has been proposed at the ELI-NP [41]. The data-based photonuclear reaction simulation algorithm was used to investigate the effects of the target dimensions and the γ-beam parameters on the specific activity for radioisotopes ^{64}Cu,^{99} Mo/^{99m}Tc, ^{225}Ra/^{225}Ac, and ^{186}Re [14, 15]. An estimation of production of medical isotopes, for example ^{99}Mo and ^{192}Ir, by photo-neutron reaction at the Canadian Light Source, has also been discussed [42].

Figure 5 shows the saturation specific activity of ^{64}Cu,^{99} Mo/^{99m}Tc,^{186} Re, and ^{225}Ra/^{225}Ac radioisotopes as a function of the target geometry for the optimized γ-beam energy as input [43]. The target thickness to be used should be 3–10 cm in order to get the maximum yield of radioisotopes. The specific activity of the radioisotopes increased along with the decrease in sizes of target thickness and radius. By using the data-based simulation code, we estimated that a saturation specific activity of the order of 1–2 mCi/g (i.e. [3.7–7.4]$\times 10^{-5}$ GBq/mg) can be achieved for thin targets (radius 1–2 mm, thickness 1 cm). In the simulation, a γ-beam flux of 10^{11} photons/s was used, which is a conservative estimate for ELI-NP. Such γ-beam flux will be achieved in the first phase of operation of the facility. In case the achieved flux shall be higher, the produced specific activities could be easily scaled, accordingly. It is suggested that the ELI-NP will present a great potential for the production of some key radioisotopes in sufficient quantities for nuclear medicine research. However, the ELI-NP cannot be, based on current estimations, a radioisotope

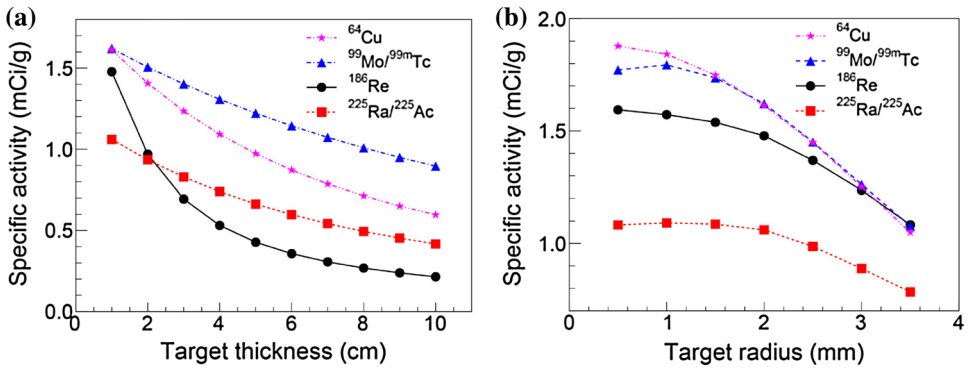

Fig. 5 Saturation specific activity of ^{64}Cu,^{99}Mo/^{99m}Tc,^{186}Re, and ^{225}Ra/^{225}Ac radioisotopes as a function of the target thickness (**a**) and radius (**b**). In Fig. 4a, an isotopic target with 2.0 mm radius was used for simulation. In Fig. 4b, an isotopic target with 1.0 cm thickness was used. The input γ-beam end-point energies are 17.6 MeV for ^{64}Cu, 14.7 MeV for ^{99}Mo/^{99m}Tc, 13.8 MeV for ^{186}Re and 12.6 MeV for ^{225}Ra/^{225}Ac [14, 15]

production facility. Such a production facility would need to provide thousands of patient doses per day and thus are much higher specific activities of 0.1 TBq. Future γ-beams facilities may have the capabilities to obtain radioisotopes with required higher activities for clinical use.

5 Conclusion and outlook

The current photonuclear model of Geant4 for photo-neutron or photo-proton production has been examined by comparisons of photonuclear cross sections of ^{9}Be,^{48}Ti, ^{133}Cs, and ^{197}Au with EXFOR in the GDR region, and by comparison of photo-neutron yield from ^{9}Be(γ,n) with that generated experimentally from an electron-bremsstrahlung source. It is found that the model of Geant4 underestimates or overestimates the experimental cross sections for photonuclear reactions. This verification shows that it is not valid within the relatively low energy region.

A data-based photonuclear reaction simulation algorithm has been demonstrated for an accurate simulation of photon-induced neutron or proton production by taking into account reliable photonuclear cross sections and attenuation effect of γ-rays interacting with target. From results of benchmarking simulations, the developed algorithm is found to reproduce well experimental data for photonuclear reactions in the GDR region. For the irradiation of bremsstrahlung photons produced by the 8.96 MeV *e*-beam on the beryllium target, resultant predictions on the yields of photo-neutrons are in accordance with experimental values. The photonuclear reaction simulation algorithm has been applied to determining the specific activity of medical radioisotopes. These radioisotopes could be produced through photonuclear reactions using the CBS γ-beam of high intensity. We suggest that the developed algorithm may have diverse applications, e.g. predictions of reaction yields required, optimizations of experimental set-up, removal of secondary effects, and various radiation shieldings.

References

1. S.E. Woosley, W.M. Howard, The p-process in supernovae. Astrophys. J. Suppl. Ser. **36**, 285–304 (1978). doi:10.1086/190501
2. S. Fujimoto, M. Hashimoto, O. Koike et al., P-process nucleosynthesis inside supernova-driven supercritical accretion disks. Astrophys. J. **585**, 418–428 (2003). doi:10.1086/345982
3. T. Hayakawa, N. Iwamoto, T. Shizuma et al., Evidence for nucleosynthesis in the supernova γ process: universal scaling for p nuclei. Phys. Rev. Lett. **93**, 161102 (2004). doi:10.1103/PhysRevLett.93.161102
4. K.W.D. Ledingham, J. Magill, P. McKenna et al., Laser-driven phototransmutation of ^{129}I—a long-lived nuclear waste product. J. Phys. D: Appl. Phys. **36**, L79–L82 (2003). doi:10.1088/0022-3727/36/18/L01
5. R. Takashima, S. Hasegawa, K. Nemoto et al., Possibility of transmutation of ^{135}Cs by ultraintense laser. Appl. Phys. Lett. **86**, 011501 (2005). doi:10.1063/1.1847715
6. E. Irani, H. Omidvar, R. Sadighi-Bonabi, Gamma rays transmutation of Palladium by bremsstrahlung and laser inverse Compton scattering. Energy Convers. Manag. **77**, 558 (2014). doi:10.1016/j.enconman.2013.09.029
7. Z.C. Zhu, W. Luo, Z.C. Li et al., Photo-transmutation of long-lived nuclear waste ^{135}Cs by intense Compton γ-ray source. Nucl. Energy, Ann. (2016). doi:10.1016/j.anucene.2015.11.017
8. K.W.D. Ledingham, P. McKenna, R.P. Singhal, Applications for nuclear phenomena generated by ultra-intense lasers. Science **300**, 1107 (2003). doi:10.1126/science.1080552
9. W. Schumaker, G. Sarri, M. Vargas et al., Measurements of high-energy radiation generation from laser-wakefield accelerated electron beams. Phys. Plasmas **21**, 056704 (2014). doi:10.1063/1.4875336
10. Z.J. Sun, D. Wells, C. Segebade et al., A comparison of various procedures in photon activation analysis with the same irradiation setup. Nucl. Instrum. Methods B **339**, 53–57 (2014). doi:10.1016/j.nimb.2014.08.021

11. V.N. Starovoitova, L. Tchelidze, D.P. Wells, Production of medical radioisotopes with linear accelerators. Appl. Radiat. Isot. **85**, 39–44 (2014). doi:10.1016/j.apradiso.2013.11.122
12. R. Avagyan, A. Avetisyan, I. Kerobyan et al., Photo-production of ^{99}Mo/^{99m}Tc with electron linear accelerator beam. Nucl. Med. Biol. **41**, 705–709 (2014). doi:10.1016/j.nucmedbio.2014.04.132
13. D. Habs, U. Köster, Production of medical radioisotopes with high specific activity in photonuclear reactions with γ-beams of high intensity and large brilliance. Appl. Phys. B: Lasers Opt. **103**, 501–519 (2011). doi:10.1007/s00340-010-4278-1
14. W. Luo, M. Bobeica, I. Gheorghe et al., Estimates for production of radioisotopes of medical interest at extreme light infrastructure—nuclear physics facility. Appl. Phys. B: Lasers Opt. **122**, 1–11 (2016). doi:10.1007/s00340-015-6292-9
15. Luo W, Production of medical radioisotope ^{64}Cu by photoneutron reaction using ELI-NP γ-ray beam. Nucl. Sci. Tech. **27**, 96 (2016). doi:10.1007/s41365-016-0094-6
16. F. Rahmani, M. Shahriari, Hybrid photoneutron source optimization for electron accelerator-based BNCT. Nucl. Instrum. Methods A **618**, 48–53 (2010). doi:10.1016/j.nima.2010.02.268
17. F. Torabi, S.F. Masoudi, F. Rahmani, Photoneutron production by a 25 MeV electron linac for BNCT application. Ann. Nucl. Energy **54**, 192–196 (2013). doi:10.1016/j.anucene.2012.11.001
18. W.L. Huang, Q.F. Li, Y.Z. Lin, Calculation of photoneutrons produced in the targets of electron linear accelerators for radiography and radiotherapy applications. Nucl. Instrum. Methods B **229**, 339–347 (2005). doi:10.1016/j.nimb.2004.12.117
19. W.L. Huang, Q.F. Li, Y.Z. Lin et al., Measurements of photoneutrons produced by a 15 MeV electron linac for radiography applications. Nucl. Instrum. Methods B **251**, 361–366 (2006). doi:10.1016/j.nimb.2006.07.018
20. M. Tatari, A.H. Ranjbar, Design of a photoneutron source based on 10 MeV electrons of radiotherapy linac. Ann. Nucl. Energy **63**, 69–74 (2014). doi:10.1016/j.anucene.2013.07.025
21. ELI-NP facility. http://www.eli-np.ro
22. W. Luo, W. Xu, Q.Y. Pan et al., X-ray generation from slanting laser-Compton scattering for future energy-tunable Shanghai laser electron gamma source. Appl. Phys. B: Lasers Opt. **101**, 761–771 (2010). doi:10.1007/s00340-010-4100-0
23. S. Agostinelli, Geant4 collaboration, GEANT4: A Simulation toolkit. Nucl. Instr. Method A **506**, 250–303 (2003). doi: 10.1016/S0168-9002(03)01368-8
24. J. Allison, K. Amako, J. Apostolakis et al., Geant4 developments and applications. IEEE Trans. Nucl. Sci. **53**, 270–278 (2006). doi:10.1109/TNS.2006.869826
25. A. Fasso, A. Ferrari, J. Ranft, P.R. Sala, in Proceedings of the FLUKA: a multi-particle transport code, CERN-2005-10(2005), INFN/TC05/11, SLAC-R-773
26. IAEA Nuclear data services. http://www-nds.iaea.org/exfor/exfor.htm
27. J.E. McFee, A.A. Faust, K.A. Pastor, Photoneutron spectroscopy using monoenergetic gamma rays for bulk explosives detection. Nucl. Instrum. Methods A **704**, 131–139 (2013). doi:10.1016/j.nima.2012.12.053
28. J.W. Shin, A data-based photonuclear reaction model for GEANT4. Nucl. Instrum. Methods B **358**, 194–200 (2015). doi:10.1016/j.nimb.2015.06.034
29. C. Sun, Y.K. Wu, Theoretical and simulation studies of characteristics of a Compton light source. Phys. Rev. ST: Accel. Beams **14**, 044701 (2011). doi:10.1103/PhysRevSTAB.14.044701
30. W. Luo, W. Xu, Q.Y. Pan et al., A 4D Monte Carlo laser-Compton scattering simulation code for the characterization of the future energy-tunable SLEGS. Nucl. Instr. Methods A **660**, 108–115 (2011). doi:10.1016/j.nima.2011.09.035
31. W. Luo, H.B. Zhuo, Y.Y. Ma et al., The nonlinear effect in relativistic Compton scattering for an intense circularly polarized laser. Phys. Scr. **89**, 075208 (2014). doi:10.1088/0031-8949/89/7/075208
32. D. Filipescu, H. Utsunomiya, I. Gheorghe et al., Geant4 simulations on Compton scattering of laser photons on relativistic electrons. AIP Conf. Proc. **1645**, 322 (2015). doi:10.1063/1.4909594
33. M. Herman, R. Capote, B.V. Carlson et al., EMPIRE: nuclear reaction model code system for data evaluation. Nucl. Data Sheets **108**, 2655 (2007). doi:10.1016/j.nds.2007.11.003
34. Koning A J, D. Rochman D. ftp://ftp.nrg.eu/pub/www/talys/tendl2010/tendl2010.html
35. NIST X-ray attenuation databases. http://physics.nist.gov/PhysRefData/XrayMassCoef/tab3.html
36. G4PhotoNuclearProcess. http://geant4.cern.ch/support/proc_mod_catalog/processes/hadronic/G4PhotoNuclearProcess.html
37. A. Heikkinen, N. Stepanov, H.P. Weillish, Bertini intra-nuclear cascade implementation in geant4. in *Proceedings of 2003 Conference for Computing in High-Energy and Nuclear Physics (CHEP 03)*, (La Jolla, 2003). http://arxiv.org/abs/nucl-th/0306008
38. K.M. Eshwarappa, G. Sanjeev, K. Siddappa et al., Comparison of photoneutron yield from beryllium irradiated with bremsstrahlung radiation of different peak energy. Ann. Nucl. Energy **34**, 896–901 (2007). doi:10.1016/j.anucene.2007.04.009
39. K.M. Eshwarappa, S.K. Ganesh et al., Estimation of photoneutron yield from beryllium target irradiated by variable energy microtron-based bremsstrahlung radiation. Nucl. Instrum. Methods A **540**, 412–418 (2005). doi:10.1016/j.nima.2004.12.001
40. H. Ejiri, T. Shima, S. Miyamoto et al., Resonant photonuclear reactions for isotope transmutation. J. Phys. Soc. Jpn. **80**, 094202 (2011). doi:10.1143/JPSJ.80.094202
41. M. Bobeica, D. Niculae, D. Balabanski et al., Radioisotope production for medical applications at ELI-NP. Rom. Rep. Phys. **68**, S847–S883 (2016)
42. B. Szpunar, C. Rangacharyulu, S. Date, H. Ejiri, Estimate of production of medical isotopes by photo-neutron reaction at the Canadian light source. Nucl. Instr. Method A **729**, 41–50 (2011). doi:10.1016/j.nima.2013.06.106
43. W. Luo, M. Bobeica, D. Filipescu et al., Production of radioisotopes of medical interest by photonuclear reaction using ELI-NP γ-ray beam. Acta Phys. Pol. B **47**, 763–769 (2016). doi:10.5506/APhysPolB.47.763